Nonlinear Dyn manuscript No.
(will be inserted by the editor)

A multiple focus-center-cycle bifurcation in 4D discontinuous piecewise linear Memristor oscillators

Enrique Ponce⋆ and Andrés Amador and Javier Ros

Received: date / Accepted: date

Abstract The dynamical richness of 4D memristor oscillators has been recently studied in several works, showing different regimes, from stable oscillations to chaos. Typically, only numerical simulations have been reported and so there is a lack of mathematical results. We focus our analysis in the existence of multiple stable oscillations in the 4D piecewise linear version of the canonical circuit proposed by M. Itoh and L. O. Chua in their paper *Memristor oscillators*, International Journal of Bifurcation and Chaos, vol. 18 (11), pp. 3183–3206, (2008). This oscillator is modeled by a discontinuous piecewise linear dynamical system.

By adding one parameter that stratifies the 4D dynamics, it is shown that the dynamics in each stratum is topologically equivalent to a 3D continuous piecewise linear dynamical system. Some previous results on bifurcations in such reduced system, allow to detect rigorously for the first time a multiple focus-center-cycle bifurcation in a three-parameter space, leading to the appearance of a topological sphere in the original model, completely foliated by stable periodic orbits.

E. Ponce (Corresponding author)
Departamento de Matemática Aplicada
Escuela Técnica Superior de Ingeniería, Sevilla, Spain
Tel.: +34-95-4486172
Fax: +34-95-4486165
E-mail: eponcem@us.es

A. Amador
Facultad de Ingeniería
Departamento de Ciencias Naturales y Matemáticas
Pontificia Universidad Javeriana, Cali, Colombia
E-mail: afamador@javerianacali.edu.co

J. Ros
Departamento de Matemática Aplicada
Escuela Técnica Superior de Ingeniería, Sevilla, Spain
E-mail: javieros@us.es

Keywords Bifurcations · Memristor oscillator · Piecewise linear systems · Periodic orbit · Boundary equilibrium bifurcation · Extreme multistability · Focus-center-limit cycle bifurcation

1 Introduction

Stan Williams and co-workers announced in the journal Nature [28] that the missing circuit element, the memristor postulated 37 years before by Leon O. Chua in [14] had been found. The memristor was defined by Chua as an electronic device characterized by a relation between the flux φ and the charge q in the form $f(\varphi, q) = 0$. Memristor is so known as the fourth basic two-terminal circuit element, where the others three are the resistance, the inductance and the capacitance.

In the paper *Memristor Oscillators* by Itoh and Chua [23] authors derive several nonlinear oscillators starting from the so-called Chua's oscillators, by replacing the Chua's diode with a memristor. They assume that the memristor is characterized by a monotone increasing and piecewise linear nonlinearity of the form

$$q(\varphi) = b \cdot \varphi + \frac{a-b}{2}\left(|\varphi+1| - |\varphi-1|\right),$$

or

$$\varphi(q) = d \cdot q + \frac{c-d}{2}\left(|q+1| - |q-1|\right),$$

where $a, b, c, d > 0$. Thus, these oscillators give rise to piecewise linear dynamical systems.

Continuous piecewise linear (CPWL, for short) systems are used in diverse areas to accurately model many physical phenomena, sometimes, involving abrupt events or fast transitions. The dynamics of a CPWL system in $\mathbb{R}^3$ with two or three zones can be rather complex. In

these systems phenomena as bistability, hysteresis, instantaneous transitions of a stable equilibrium to chaotic attractor, and the existence of the invariant cones have been shown [7,11,19,21,22,27].

When memristors oscillators with CPWL characteristics are modeled in the usual current-voltage setting, the lack of smoothness, leads to discontinuous piecewise linear dynamical systems. Such discontinuities make difficult to get mathematical proofs about their dynamics. Thus, many authors have described numerically the presence of periodic orbits and chaotic behavior (see for instance [3,4,12,16,24,31,34]). In particular, for memristor oscillators with a dimension greater than or equal to four, cases of extreme multistability leading to coexistence of an infinite number of attractors are reported [5,13,30,32,33]. However, a rigorous mathematical proof of these phenomena is lacking.

In [2,25] authors provide for the first time rigorous mathematical results regarding the rich dynamics of 3D piecewise linear memristor oscillators. In this paper we consider the so called canonical 4D piecewise linear memristor oscillators given in [23] and report for the first time some mathematical results regarding the dynamics of such devices.

We present in section 2 the mathematical model of the 4D memristor oscillator under study, showing first that the involved discontinuities do not require the resort to Filippov's theory. In fact, the system possesses a family of continuous piecewise linear manifolds that are invariant under its dynamics, see Theorem 1. Furthermore, it is shown that all the parameters in the model are not essential, see Proposition 1.
In section 3, we present the main results of this work. It turns out that on any invariant set the dynamics can be described by a 3D continuous piecewise linear system, so that, coming back to the original 4D memristor oscillator, it can be said that the dynamics is essentially three-dimensional and falsely discontinuous. See Theorem 2 and Proposition 2. It is also shown how to pass from solutions of the reduced 3D systems to the solutions of the original 4D model, see Proposition 3. This result becomes out very useful in avoiding numerical difficulties when one tries to simulate the dynamics of the model by using the original vector field.

Once obtained the 3D system that reproduces the dynamics on any invariant manifold, we study the number of equilibria and their geometrical location, see Proposition 4. For these system is by no means trivial to justify the existence of periodic orbits. However, by resorting to some previous results regarding the focus-center-limit cycle bifurcation [8,20–22], it is possible to guarantee the existence of limit cycles in certain regions of the basic three-parameter space. See Theorems 3, 4 and 5. The main contribution of the work is summarized in Theorem 6. For the first time it is reported a multiple focus-center-cycle bifurcation (MFCC bifurcation) leading to the sudden appearance of a bounded hypersurface foliated by stable periodic orbits in the original 4D memristor oscillator. Finally, section 4 is dedicated to illustrate numerically the dynamical richness of the 3D reduced system, by considering cases that require further investigation.

2 Modeling of the oscillator

We consider the canonical fourth-order memristor oscillator given in [23], see Figure 1, where a flux-controlled memristor is the only nonlinear element. Applying Kirchhoff's laws to the upper nodes and the central loop we obtain the equations

$$i_1 = i_3 - i, \quad v_3 = v_2 - v_1, \quad i_2 = -i_3 + i_4,$$

where v_1, v_2 are the voltage across the capacitors C_1, C_2 respectively, and v_3 is the voltage across the inductance. Similarly, the current i_1, i_2, i_3 and i are as shown in Figure 1. Taking into account the different dipoles, and in particular that the current through the memristor satisfies

$$i = \frac{dq}{dt} = \frac{dq}{d\varphi}\frac{d\varphi}{dt},$$

it is then possible to arrive at the equations

$$\begin{aligned} C_1\frac{dv_1}{d\tau} &= i_3 - W(\varphi)v_1,\\ L\frac{di_3}{d\tau} &= v_2 - v_1,\\ C_2\frac{dv_2}{d\tau} &= -i_3 + Gv_2,\\ \frac{d\varphi}{d\tau} &= v_1, \end{aligned} \tag{1}$$

where C_1, C_2 denote the capacitance of the capacitors, L is the inductance of the inductor, the conductance has a negative value $-G$, $W(\varphi) = \frac{dq}{d\varphi}$ and φ denote the flux across the memristor, see section 3.1 of [23] for more details. Taking $L = 1$ as in the quoted paper, system (1) can be written as

$$\begin{aligned} \frac{dx}{d\tau} &= \alpha y - \alpha W(w)x,\\ \frac{dy}{d\tau} &= z - x,\\ \frac{dz}{d\tau} &= -\beta y + \gamma z,\\ \frac{dw}{d\tau} &= x, \end{aligned} \tag{2}$$

where $\alpha = 1/C_1 > 0$, $\beta = 1/C_2 > 0$, $\gamma = G/C_2 > 0$ and

$$W(w) = \frac{dq(w)}{dw}, \tag{3}$$

being q the characteristics of the flux-controlled memristor. The new state variables are $x = v_1$ (voltage across the first capacitor); $y = i_3$ (current across the inductor L); $z = v_2$ (voltage across the second capacitor) and $w = \varphi$, the flux of the memristor.

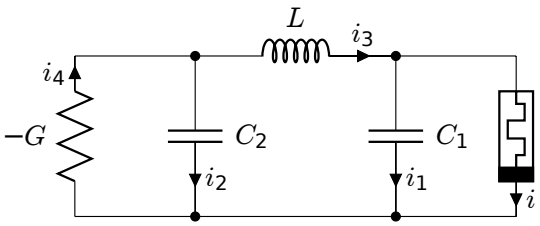

Fig. 1 A fourth-order canonical memristor oscillator.

Remark 1 The continuous function of the flux-charge characteristics $q(w)$ is sometimes assumed to be in the set $\mathcal{PC}^1(\mathbb{R})$ of continuous piecewise-smooth functions. Then, the vector field (2) becomes a discontinuous vector field at certain hyperplanes $w = w_i$ for a finite set of values w_i where $q(w)$ is not differentiable. In fact, assuming that we could compute the two lateral limits

$$W_i^+ = \lim_{w \to w_i^+} W(w), \quad W_i^- = \lim_{w \to w_i^-} W(w),$$

at the manifold $w = w_i$, we should have the interaction of two different vector fields. However, this is not a real problem regarding the existence and uniqueness of solutions as long as such two vector fields share the normal component $\dot{w} = x$. Effectively, we can concatenate solutions in the natural way and so they become functions in $\mathcal{PC}^1(\mathbb{R})$, which exist for any $t \in \mathbb{R}$ and are uniquely defined. Therefore, here is not needed at all to invoke Filippov's theory [18].

Following a similar procedure to the one done in [2] and [25], it is easy to conclude the following result.

Theorem 1 *Consider system* (2) *where* $q \in \mathcal{PC}^1(\mathbb{R})$ *is given and the (possibly discontinuous) function* W *is defined as in* (3)*. If we introduce the continuous function*

$$H(x, y, z, w) := \beta\,(x + \alpha q(w)) - \alpha\gamma\,(y + w) + \alpha z, \tag{4}$$

then for any $h \in \mathbb{R}$ *the set*

$$S_h = \{(x, y, z, w) \in \mathbb{R}^4 : H(x, y, z, w) = h\}, \tag{5}$$

is an invariant manifold for the system. Therefore, system (2) *has an infinite family of invariant manifolds foliating the whole* $\mathbb{R}^4$*, and so the dynamics is essentially three-dimensional.*

The existence of the conserved quantity H has a precise physical meaning for the original system (1). In fact, we get from (4)

$$C_1C_2\frac{dH}{d\tau} = C_1\frac{dv_1}{d\tau} - G\left(\frac{di_3}{d\tau} + \frac{d\varphi}{d\tau}\right) + C_2\frac{dv_2}{d\tau} + \frac{dq}{d\tau} = 0,$$

that is, $i_{C_1} + i_G + i_{C_2} + i_M = 0$ which is by no means different of the current Kirchhoff law applied to the ground node of the circuit, see section 3.1 of [23]. Thus, we deduce in this case that the conserved quantity is directly related to the conservation law for the total charge.

In the next result, we show that the parameter α is not essential and can be eliminated in system (2), alleviating the notation. Its proof is a direct computation which is omitted.

Proposition 1 *The change of time, variables and parameters*

$$\begin{aligned} &\tilde{\tau} = \alpha^{1/2}\tau,\ \tilde{x} = \alpha^{-1/2}x,\ \tilde{y} = y,\ \tilde{z} = \alpha^{-1/2}z,\\ &\tilde{\beta} = \alpha^{-1/2}\beta,\ \tilde{\gamma} = \alpha^{-1/2}\gamma,\ \tilde{a} = \alpha^{1/2}a,\ \tilde{b} = \alpha^{1/2}b, \end{aligned} \tag{6}$$

transforms system (2) *into the form*

$$\begin{aligned} \frac{dx}{d\tau} &= y - W(w)x,\\ \frac{dy}{d\tau} &= z - x,\\ \frac{dz}{d\tau} &= -\beta y + \gamma z,\\ \frac{dw}{d\tau} &= x, \end{aligned} \tag{7}$$

where the tildes for the time, new variables and parameters have been removed for the sake of simplicity.

For convenience, we will rewrite system (7) as

$$\begin{aligned} \dot{y}_1 &= y_4,\\ \dot{y}_2 &= y_3 - y_4,\\ \dot{y}_3 &= -\beta y_2 + \gamma y_3,\\ \dot{y}_4 &= y_2 - W(y_1)y_4, \end{aligned} \tag{8}$$

where $(y_1, y_2, y_3, y_4) = (w, y, z, x)$. Note that the function H given in (4) can be rewritten now as

$$H(y_1, y_2, y_3, y_4) = \beta\,(y_4 + q(y_1)) - \gamma\,(y_1 + y_2) + y_3, \tag{9}$$

and so in the new variables we have the invariant manifolds

$$S_h = \{(y_1, y_2, y_3, y_4) \in \mathbb{R}^4 : H(y_1, y_2, y_3, y_4) = h\}. \tag{10}$$

The equilibrium points of system (8) are given by the unbounded set formed by all points in the y_1-axis, namely

$$E = \{(y_1, y_2, y_3, y_4) \in \mathbb{R}^4 : y_2 = y_3 = y_4 = 0, y_1 \in \mathbb{R}\}.$$

It should be noticed that all these equilibria have an eigenvalue $\lambda = 0$, since their linearization matrix has a null first column.

3 Main results

The following result exploits the fact that the dynamics is always confined to a certain invariant manifold S_h. We show that, by a suitable change of variables, a topologically equivalent system with a dimensional reduction and without discontinuities is achieved. The price to be payed is the introduction of an additional parameter associated to the chosen level set S_h defined in (5). For all the proofs of the results of this section see section 5.

Theorem 2 *Consider system* (8) *with* $\beta \neq 0$ *and* $q \in \mathcal{PC}^1(\mathbb{R})$. *On any invariant set* S_h *the dynamics of the system is topologically equivalent to the dynamics of the continuous system*

$$\begin{aligned}
\dot{x}_1 &= \frac{\gamma}{\beta}(x_1 + x_2) - q(x_1) - \frac{1}{\beta}x_3 + \frac{h}{\beta},\\
\dot{x}_2 &= x_3 - \frac{\gamma}{\beta}(x_1 + x_2) + q(x_1) + \frac{1}{\beta}x_3 - \frac{h}{\beta},\\
\dot{x}_3 &= -\beta x_2 + \gamma x_3.
\end{aligned} \tag{11}$$

Note that $\dot{x}_1 + \dot{x}_2 = x_3$, so that, equilibria of system (11) satisfy $x_2 = x_3 = 0$, and the equation

$$\beta q(x_1) - \gamma x_1 = h, \tag{12}$$

so that generically, we will have a finite number of equilibria for each $h \in \mathbb{R}$. In what follows, we consider the function q as the continuous piecewise linear function defined by

$$q(x) = \begin{cases} b(x-1) + a, & \text{if} \quad x > 1,\\ ax, & \text{if} \quad |x| \leqslant 1,\\ b(x+1) - a, & \text{if} \quad x < -1, \end{cases} \tag{13}$$

so that

$$W(x) = \frac{dq(x)}{dx} = \begin{cases} b, & \text{if} \quad |x| > 1,\\ a, & \text{if} \quad |x| < 1. \end{cases} \tag{14}$$

As a consequence, the invariant manifolds S_h given in (10) are continuous and piecewise linear (CPWL, for short).

Remark 2 According to Remark 1, for the particular case of piecewise linear function (13) leading to (14), the discontinuous system (8) has two discontinuity manifolds, namely $y_1 = \pm 1$. Since they are parallel, we cannot have boundary intersection bifurcations. Moreover, in each of these discontinuity hyperplanes the two contiguous vector fields share the orthogonal component to such hyperplane. Therefore, there are no sliding sets at all, and so we can discard all the discontinuity induced bifurcations involving sliding motions. In particular, adding-sliding, crossing-sliding, grazing-sliding and switching-sliding bifurcations are not possible. In fact, from Theorem 2 we see that the dynamics can be described by a continuous system, so that system (8) could be termed as false discontinuous.

For the subsequent analysis of system (11), it turns out very useful to resort to the so called generalized canonical Liénard's canonical form, as follows.

Proposition 2 *Consider the fourth-order discontinuous system* (8) *with* $\beta \neq 0$ *and the function* q *defined as in* (13). *On any invariant CPWL manifold* S_h *given in* (10), *the system is topologically equivalent to the third-order continuous canonical system*

$$\dot{\mathbf{x}} = \begin{pmatrix} t_E & -1 & 0\\ m_E & 0 & -1\\ d_E & 0 & 0 \end{pmatrix}\mathbf{x} + \begin{pmatrix} t_C - t_E\\ m_C - m_E\\ d_C - d_E \end{pmatrix} \operatorname{sat}\left(\mathbf{e}_1^T\mathbf{x}\right) + \frac{h}{\beta}\begin{pmatrix} 1\\ \gamma\\ \beta \end{pmatrix} \tag{15}$$

where $t_{C,E}$, $d_{C,E}$ *and* $m_{C,E}$ *are given by*

$$\begin{aligned}
&t_C = \gamma - a, \quad m_C = 1 + \beta - \gamma a, \quad d_C = \gamma - \beta a,\\
&t_E = \gamma - b, \quad m_E = 1 + \beta - \gamma b, \quad d_E = \gamma - \beta b.
\end{aligned} \tag{16}$$

The numerical simulation of system (8) is prone to numerical errors, associated with the presence of infinite number of piecewise linear invariant manifold S_h. Thus, we need to implement a safeguard that force the solutions of system (8) to stay at the corresponding invariant manifold S_h. The next result avoids the numerical difficulties because we give for any solution of the continuous canonical system (15)-(16) with a given value of h the corresponding solution of the discontinuous system (8).

Proposition 3 *Given* $h \in \mathbb{R}$ *and* $\beta \neq 0$, *if the vector* $(x_1(\tau), x_2(\tau), x_3(\tau)) \in \mathbb{R}^3$ *is a solution of canonical system* (15)-(16), *then*

$$\mathbf{y}(\tau) = \begin{pmatrix} x_1(\tau)\\ (\gamma^2 - \beta - 1)x_1(\tau) - \gamma x_2(\tau) + x_3(\tau)\\ (\gamma^3 - 2\beta\gamma)x_1(\tau) + (\beta - \gamma^2)x_2(\tau) + \gamma x_3(\tau)\\ \gamma x_1(\tau) - x_2(\tau) - q(x_1(\tau)) + h/\beta \end{pmatrix}$$

(17)

is a solution of discontinuous system (8) *on* S_h*, where the function* q *is defined as in* (13).

Following the terminology introduced in section 5.1.1 of [6], in the next result we study, by taking h as a bifurcation parameter, the boundary-equilibrium bifurcation (BEB, for short) of system (15)-(16). Such bifurcation can be of two different types, namely persistence (the number of equilibria does not change) and non-smooth fold, when the number of equilibria changes by two. The non-generic cases $d_C = 0$ or $d_E = 0$ are excluded for brevity

Proposition 4 *The following statements hold for canonical system* (15)-(16) *with* $\beta \neq 0$.

(a) If $d_C \cdot d_E > 0$ *the system has for any* $h \in \mathbb{R}$ *only one real equilibrium point so that for* $h = \pm d_C$ *we have a persistence BEB, see figure 2 (a).*

(b) If $d_C \cdot d_E < 0$ *the system has for* $|h| > |d_C|$ *only one real equilibrium point and for* $|h| < |d_C|$ *three real equilibrium points. Therefore, for* $h = \pm d_C$ *the system has two equilibrium points and a non-smooth fold BEB, see figure 2 (b).*

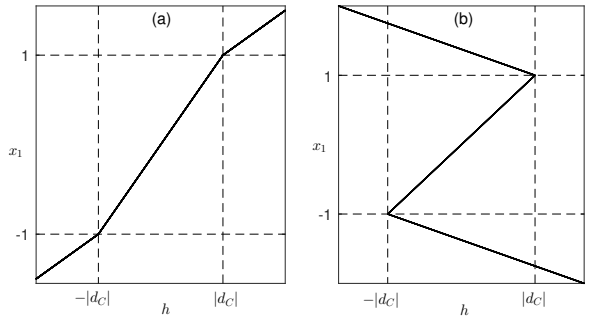

Fig. 2 Real equilibrium points of canonical system (15)-(16) with respect to the parameter h for the case $d_C < 0$. (a) Taking $d_E < 0$, statement (a) of Proposition 4 shows persistence BEB's at $h = \pm d_C$. (b) Taking $d_E > 0$, statement (b) of Proposition 4 shows non-smooth fold BEB's at $h = \pm d_C$.

The equilibria of system (15)-(16) are of the form $(x_1, 0, 0)$ where x_1 is a solution of (12). When $|x_1| < 1$ the stability of such equilibrium is determined by the roots of the polynomial $\lambda^3 - t_C\lambda^2 + m_C\lambda - d_C$. These equilibria can undergo the so-called focus-center-limit cycle (FCLC, for short) bifurcation [20,21,8,22] under the conditions

$$m_C > 0, \quad m_C t_C = d_C. \tag{18}$$

Such conditions assure that the matrix A_C has a pair of pure imaginary eigenvalues. Effectively, under the hypothesis of the existence of a complex eigenvalue pair, if we introduce the parameter $\varepsilon = m_C t_C - d_C$, then we conclude that it is associated to the sign of the real part of such complex eigenvalues. Effectively, if λ, and $\sigma \pm i\omega$ are the three eigenvalues a straightforward computation gives

$$\varepsilon = m_C t_C - d_C = 2\sigma\left[(\sigma+\lambda)^2 + \omega^2\right].$$

Therefore, for $\varepsilon = 0$ we have a linear center in the central zone on the corresponding focal plane. Since $d_C = \lambda(\sigma^2 + \omega^2)$, we observe that when $d_C < 0$, such focal plane is attractive because we have a dynamics approaching the plane along the transversal direction associated to the λ-eigenvector.

Assuming β fixed, we start by analyzing the auxiliary expression $\varepsilon(a, \gamma) = m_C t_C - d_C$ that leads to the bifurcation when it vanishes, where m_C, t_C and d_C are given in (16). We have

$$\varepsilon(a, \gamma) = a^2\gamma - a\gamma^2 + \beta\gamma - a. \tag{19}$$

For $\beta = 1$ we get $\varepsilon(a, \gamma) = (1 - a\gamma)(\gamma - a)$. If $\gamma = a$ then we have $t_C = d_C = 0$, so that we do not have any equilibrium point for $h \neq 0$; anyway, $m_C = 2 - a^2$, and so for $|a| < \sqrt{2}$ we get a Hopf-zero bifurcation if $h = 0$, see [26]. The other possibility given by $\gamma = 1/a$ is not so problematic but we will not consider anymore the case $\beta = 1$, as it is a non-generic situation, to be investigated elsewhere. For $\beta \neq 1$, the condition $\varepsilon(a, \gamma) = 0$ is equivalent to the equality $a\gamma(a - \gamma) = a - \beta\gamma$, which is only possible for $a\gamma > 0$. Effectively, if $a\gamma < 0$, then

$$\operatorname{sgn}(a - \gamma) = \operatorname{sgn}(a - \beta\gamma)$$

and the previous equality can not be fulfilled. Therefore, the points where (19) vanishes are in the first or third quadrant of the parameter plane (a, γ). In Figure 3, we show for the first quadrant of parameter plane the locus $\varepsilon(a, \gamma) = 0$, which is formed by two disconnected branches. As will be later detailed, not all the points in such branches are FCLC bifurcation points. See Theorems 4 and 5, below.

We observe that system (15)-(16) is invariant under the symmetry

$$(x, y, x, h) \to (-x, -y, -z, -h), \tag{20}$$

so that for the analysis of the FCLC bifurcation, we only need to consider the dynamics of the system for $h \geq 0$. When $h = 0$ the vector field of the system is indeed symmetric, and then for the equilibrium at the origin Theorem 1.1 of [20] on the FCLC bifurcation applies. This result assures under certain hypotheses,

to be detailed later, the bifurcation of a limit cycle from a linear center configuration that exists at the critical bifurcation value in the central zone.
When $0 < h < |d_C|$ the only equilibrium of system (15)-(16) in the central zone is not at the origin any longer, but is nearer to one of the two planes $x = \pm 1$, see Figure 2. Then a similar FCLC Theorem applies (see Theorem 1 of [8]) that involves two linear zones.
We note that the FCLC bifurcation condition (18) does not depend on the concrete value of h, so that the FCLC bifurcation takes place simultaneously for all values of $|h| < |d_C|$. Therefore, we can state as a consequence the following result, where a new criticality parameter ρ is introduced to characterize the bifurcation.

Theorem 3 *Consider the canonical system* (15)-(16) *with* $|h| < |d_C| \neq 0$, $m_C > 0$, $\varepsilon = m_C t_C - d_C$, *and the non-degeneracy parameter*

$$\rho = d_C m_C - d_C m_E + d_E m_C - m_C^2 t_E. \tag{21}$$

Then, for $\rho \neq 0$ *and* $\varepsilon = 0$ *the system undergoes a focus-center-limit cycle bifurcation; that is, from the lineal center configuration in the central zone, which exists for* $\varepsilon = 0$, *one limit cycle appears for* $\varepsilon\rho > 0$ *and* ε *sufficiently small. In particular, if* $\rho > 0$ *and* $d_C < 0$, *then the limit cycle bifurcates for* $\varepsilon > 0$ *and is orbitally asymptotically stable. Otherwise, if* $\rho < 0$ *or* $d_C > 0$ *the bifurcating limit cycle is unstable, being completely unstable when both inequalities hold.*

In all the cases, the bifurcating limit cycle comes from the most external periodic orbit of the linear center that exist for $\varepsilon = 0$, which is tangent to one of the planes $\mathbf{e}_1^T\mathbf{x} = \pm 1$ or to both of them if $h = 0$.
Now, given the value of h, the FCLC bifurcation is characterized in the parameter plane (a, γ), see Figure 3. The golden ratio $\phi = (1+\sqrt{5})/2$ appears in some statements.We start by defining the auxiliary well-defined functions

$$a_{\pm}(\gamma) = \frac{\gamma^2+1}{2\gamma} \pm \sqrt{\left(\frac{\gamma^2+1}{2\gamma}\right)^2 - \beta}, \tag{22}$$

for $0 < \beta < 1$, and

$$\gamma_{\pm}(a) = \frac{\beta+a^2}{2a} \pm \sqrt{\left(\frac{\beta+a^2}{2a}\right)^2 - 1}, \tag{23}$$

for $\beta > 1$, see Figure 3.

In the next theorem we give a complete characterization of the FCLC bifurcation for $0 < a < b$.

Theorem 4 *Consider the reduced system* (15)-(16) *with* $|h| < |d_C| \neq 0$, $0 < a < b$, $\beta \neq 1$, *and* $\gamma > 0$. *Additionally, consider the functions* $a_{\pm}(\gamma)$ *and* $\gamma_{\pm}(a)$ *defined in* (22)-(23) *respectively. The following statements hold.*

(a) If $0 < \beta < 1$ *then at the points* $(a, \gamma) = (a_-(\gamma), \gamma)$ *the system undergoes a FCLC bifurcation, so that an unstable limit cycle bifurcates for* $a < a_-(\gamma)$.
(b) If $0 < \beta < 1$ *then at the points* $(a, \gamma) = (a_+(\gamma), \gamma)$ *with* $\gamma < \sqrt{\beta(1+\beta)}$ *the system undergoes a FCLC bifurcation, so that an unstable limit cycle bifurcates for* $a < a_+(\gamma)$.
(c) If $\beta > 1$ *then at the points* $(a, \gamma) = (a, \gamma_-(a))$ *with* $a < \sqrt{\beta}$ $(a > \sqrt{\beta})$ *the system undergoes a FCLC bifurcation, so that a stable (unstable) limit cycle bifurcates for* $\gamma > \gamma_-(a)$ $(\gamma < \gamma_-(a))$.
(d) If $1 < \beta < \phi$ *then at the points* $(a, \gamma) = (a, \gamma_+(a))$ *with* $a < \sqrt{\beta}$ $(\sqrt{\beta} < a < \sqrt{(1+\beta)/\beta})$ *the system undergoes a FCLC bifurcation, so that an unstable (completely unstable) limit cycle bifurcates for* $\gamma < \gamma_+(a)$ $(\gamma > \gamma_+(a))$.
(e) If $\beta \geq \phi$ *then at the points* $(a, \gamma) = (a, \gamma_+(a))$ *with* $a < \sqrt{(1+\beta)/\beta}$ *the system undergoes a FCLC bifurcation, so that an unstable limit cycle bifurcates for* $\gamma < \gamma_+(a)$.

In all the above cases, the system has for the critical values of parameters indicated a linear center in the region $|\mathbf{e}_1^T\mathbf{x}| \leq 1$ *and the limit cycle bifurcates from the most external periodic orbit of the center.*

A similar result can be stated for $0 < b < a$.

Theorem 5 *Consider the reduced system* (15)-(16) *with* $|h| < |d_C| \neq 0$, $0 < b < a$, $\beta \neq 1$, *and* $\gamma > 0$. *Additionally, consider the functions* $a_{\pm}(\gamma)$ *and* $\gamma_{\pm}(a)$ *defined in* (22)-(23) *respectively. The following statements hold.*

(a) If $0 < \beta < 1$ *then at the points* $(a, \gamma) = (a_-(\gamma), \gamma)$ *the system undergoes a FCLC bifurcation, so that a completely unstable limit cycle bifurcates for* $a > a_-(\gamma)$.
(b) If $0 < \beta < 1$ *then at the points* $(a, \gamma) = (a_+(\gamma), \gamma)$ *with* $\gamma < \sqrt{\beta(1+\beta)}$ *the system undergoes a FCLC bifurcation, so that a stable limit cycle bifurcates for* $a > a_+(\gamma)$.
(c) If $\beta > 1$ *then at the points* $(a, \gamma) = (a, \gamma_-(a))$ *with* $a < \sqrt{\beta}$ $(a > \sqrt{\beta})$ *the system undergoes a FCLC bifurcation, so that an unstable (stable) limit cycle bifurcates for* $\gamma < \gamma_-(a)$ $(\gamma > \gamma_-(a))$.
(d) If $1 < \beta < \phi$ *then at the points* $(a, \gamma) = (a, \gamma_+(a))$ *with* $a < \sqrt{\beta}$ $(\sqrt{\beta} < a < \sqrt{(1+\beta)/\beta})$ *the system undergoes a FCLC bifurcation, so that an completely unstable (unstable) limit cycle bifurcates for* $\gamma < \gamma_+(a)$ $(\gamma > \gamma_+(a))$.
(e) If $\beta \geq \phi$ *then at the points* $(a, \gamma) = (a, \gamma_+(a))$ *with* $a < \sqrt{(1+\beta)/\beta}$ *the system undergoes a FCLC bifurcation, so that an unstable limit cycle bifurcates for* $\gamma < \gamma_+(a)$.

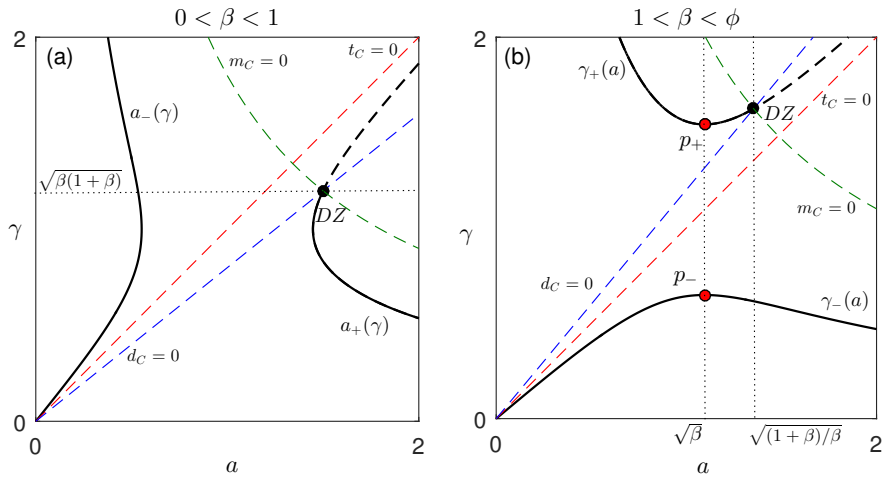

Fig. 3 The thin dashed lines represents the locus $t_C = 0$ (red), $d_C = 0$ (blue) and $m_C = 0$ (green). The thick black curves corresponds to FCLC bifurcation points, excepting the dashed points where $m_C < 0$. The panel (a) it is shown the case $0 < \beta < 1$ ($\beta = 0.8$), while in (b) there appears the case $\beta < 1$ ($\beta = 1.2$).

In all the above cases, the system has for the critical values of parameters indicated a linear center in the region $|\mathbf{e}_1^T \mathbf{x}| \leq 1$ *and the limit cycle bifurcates from the most external periodic orbit of the center.*

In Figure 3, we give a schematic view of the different FCLC bifurcations predicted by Theorems 4 and 5. We denote by s,u,cu the stable, unstable and completely unstable character of the bifurcating limit cycle. The arrows across the branches of the curve $\varepsilon(a,\gamma) = 0$ denote the reported bifurcations.

Next, we give our last main result for the 4D discontinuous system (8), which emphasizes three cases of simultaneous appearance of an infinite number of stable periodic orbits in what can be called a multiple focus-center-cycle (for short, MFCC) bifurcation. This bifurcation, to be reported for the first time up to the best of our knowledge, is a consequence of the standard focus-center-limit cycle bifurcations that occur in such invariant CPWL manifold S_h for the values of h with $|h| < |d_C|$. Note that the multiple stable oscillations that are predicted cannot be called limit cycles as long as they are non isolated when one thinks of the 4D system (8).

Theorem 6 *Consider the discontinuous system* (8) *with* $\beta \neq 1$. *Additionally, consider the functions* a_+ *and* γ_- *defined in* (22)-(23) *respectively. The following statements hold.*

(a) If $\beta > 1$, $a < \sqrt{\beta}$ *and* $0 < a < b$ *then for* $\gamma = \gamma_-(a)$ *the system undergoes a MFCC bifurcation, so that when* $\gamma \leq \gamma_-(a)$ *all the equilibria in central segment are stable, becoming unstable for* $\gamma > \gamma_-(a)$. *When* $\gamma = \gamma_-(a)$ *there appears a bounded, simply connected set, symmetric with respect to the origin and completely full of periodic orbits that surrounds such set of central equilibria. For* $\gamma - \gamma_-(a) > 0$ *and sufficiently small, the above set of periodic orbits disappears giving rise to a bounded hypersurface* $\Omega \subset \mathbb{R}^4$ *foliated by stable periodic orbits.*

(b) If $0 < \beta < 1$, $\gamma < \sqrt{\beta(1+\beta)}$ *and* $0 < b < a$ *then for* $a = a_+(\gamma)$ *the system undergoes a MFCC bifurcation, so that when* $a \leq a_+(\gamma)$ *all the equilibria in central segment are stable, becoming unstable for* $a > a_+(\gamma)$. *When* $a = a_+(\gamma)$ *there appears a bounded, simply connected set, symmetric with respect to the origin and completely full of periodic orbits that surrounds such set of central equilibria. For* $a - a_+(\gamma) > 0$ *and sufficiently small, the above set of periodic orbits disappears giving rise to a bounded hypersurface* $\Omega \subset \mathbb{R}^4$ *foliated by stable periodic orbits.*

(c) If $0 < \beta < 1$, $a > \sqrt{\beta}$ *and* $0 < b < a$ *then for* $\gamma = \gamma_-(a)$ *the system undergoes a MFCC bifurcation, so that when* $\gamma \leq \gamma_-(a)$ *all the equilibria in central segment are stable, becoming unstable for* $\gamma > \gamma_-(a)$. *When* $\gamma = \gamma_-(a)$ *there appears a bounded, simply connected set, symmetric with respect to the origin and completely full of periodic orbits that surrounds such set of central equilibria. For* $\gamma - \gamma_-(a) > 0$ *and sufficiently small, the above set of periodic orbits disappears giving rise to a bounded hypersurface* $\Omega \subset \mathbb{R}^4$ *foliated by stable periodic orbits.*

In Figure 5, we show the effect of the reported MFCC bifurcation on system (8). Before the bifurcation we have stable equilibria (Figure 5(a)) in the central seg-

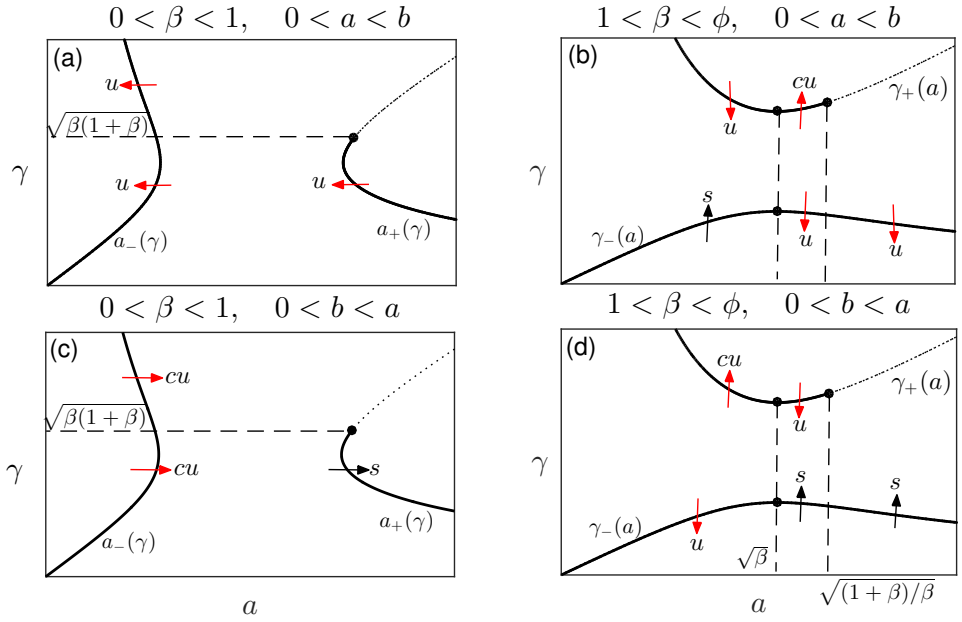

Fig. 4 Scheme of the bifurcations reported in Theorems 4 and 5. Panels (a) and (b) correspond to Theorem 4, while panels (c) and (d) to Theorem 5.

ment. After Figure 5(b), these equilibria are unstable with a sudden appearance of a hypersurface of stable periodic orbits.

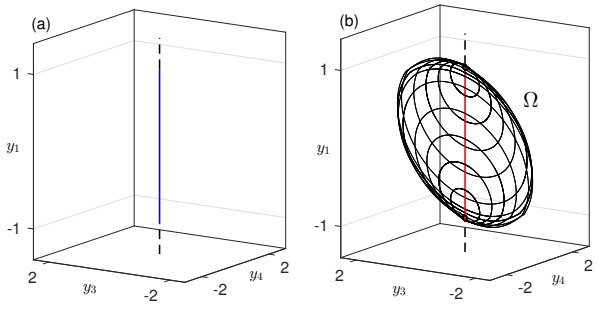

Fig. 5 The MFCC bifurcation predicted by Theorem 6(a) in the discontinuous system (8). In panel (a) points in the blue line correspond to the stable equilibria in the central zone. In panel (b) for $\gamma > \gamma_-(a)$, we show the 3D projection of some slices of the hypersurface Ω that bifurcate from the multiple center when $\gamma = \gamma_-(a)$. Parameters are $\beta = 1.2$, $a = 0.8$, $\gamma = \gamma_-(a) + 0.02$, $b = 2$. The equilibrium points of the system are unstable in all zones, the red line shows the unstable equilibria in the central zone.

To finish this section, we want to emphasize the usefulness of the 3D reduced models in order to justify the complex dynamics to be found in the 4D original models. In fact, we show in the next section other dynamics which are still needed of further analysis.

4 Numerical examples

Just to demonstrate the dynamical richness of these memristor oscillators, we select two numerical examples. In the first example, we show another case of the existence of hypersurfaces of periodic orbits, this time related to boundary equilibrium bifurcations (BEB). Furthermore, we also show a case where have detected a h-route to chaos in the reduced model.

4.1 Non-smooth fold BEB with unstable zones and stable periodic orbits.

Consider system (15)-(16) with parameters

$$\beta = 0.5, \quad \gamma = 0.325, \quad a = 0.2, \quad b = 3.5. \tag{24}$$

In this case, the system has the linear invariants $t_C = 0.125$, $d_C = 0.225$, $t_E = -3.175$, $d_E = -1.425$ and the eigenvalues of matrices $A_{C,E}$ are $\lambda_{C,E} \in \mathbb{R}$ and $\sigma_{C,E} \pm i\omega_{C,E}$ given by

$$\lambda_C = 0.1562624, \quad \sigma_C = -0.0156312,$$
$$\omega_C = 1.1998503298,$$
$$\lambda_E = -3.2008358, \quad \sigma_E = 0.0129179,$$
$$\omega_E = 0.6671051.$$

From Propositions 4 and 7 the system has for $|h| > d_C$ only one unstable real equilibrium point and for $|h| < d_C$ three unstable real equilibrium points and at $h = \pm d_C$ we have a non-smooth fold BEB of unstable

equilibrium points. In Figure 6, we have in dashed red line the real equilibrium points. When $h = \pm d_C$ a stable periodic orbit is created and for $|h| < |d_C|$ two stable periodic orbits coexist.

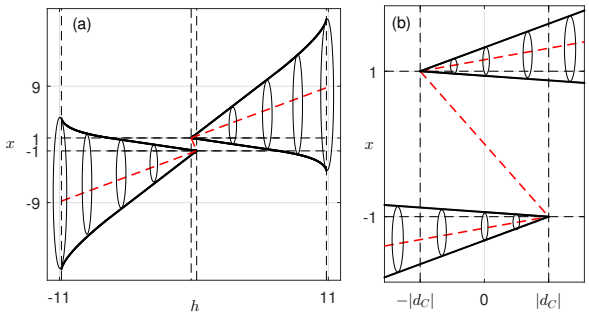

Fig. 6 (a) Bifurcation diagram of system (15)-(16) respect to parameter h. The dashed red line represents the coordinate x of the real unstable equilibrium points. For stable periodic orbits, some schematic projection joining its minimum and maximum x-values are plotted. The remaining parameters are as in (24). (b) The zoomed central region of the bifurcation diagram in (a).

From Proposition 3 this set of periodic orbits can be translated to the 4D original model leading to certain hypersurface foliated by periodic orbits. Although the lack of theoretical results for these BEB precludes at this moment any non-numerical justification, we can advance that it is possible to show the sudden appearance of these hypersurfaces in a MFCC bifurcation similar to the one included in this paper. This will be the subject of future work.

4.2 Route to chaos without parameters

In section 3.1 of [23], authors consider the discontinuous system (2) with the function q defined as in (13). They detect numerically a chaotic attractor for the set of parameters $\alpha = 4$, $\beta = 1$, $\gamma = 0.65$, $a = 0.2$ and $b = 10$. The change of variables given in (6) transforms the system into the form (15)-(16) where the new parameters are given by

$$\beta = 0.5, \quad \gamma = 0.325, \quad a = 0.4, \quad b = 20. \tag{25}$$

For these parameters we obtain the linear invariants $t_C = -0.075$, $d_C = 0.125$, $t_E = -19.675, d_E = -9.675$ and the eigenvalues of matrices $A_{C,E}$ are $\lambda_{C,E} \in \mathbb{R}$ and $\sigma_{C,E} \pm i\omega_{C,E}$ given by

$$\begin{aligned}
&\lambda_C = 0.09025818, \quad \sigma_C = -0.0826290,\\
&\omega_C = 1.17392007,\\
&\lambda_E = -19.949936, \quad \sigma_E = 0.13746820,\\
&\omega_E = 0.68269059.
\end{aligned}$$

From Propositions 4 and 7 the system has for $|h| > d_C$ only one unstable real equilibrium point and for $|h| < d_C$ three unstable real equilibrium points. As in the previous example, and at $h = \pm d_C$ we have a non-smooth fold BEB of unstable equilibrium points.

Following [29], by computing the Poincaré map on the plane $x = 1$, and taking h as the bifurcation parameter of system (15)-(16), we obtain the numerical bifurcation diagram given in Figure 7(a).
We observe that the system undergoes several period-doubling bifurcations, see the corresponding periodic orbits of Figure 7 (b),(c),(d). Finally, for $h_0 = 0$ the system has a symmetric pair strange attractors of two zones, see Figure 7(e).

Since the parameter h is not present in the original model, but it is associated to the initial conditions, we can speak of a route to chaos without parameters or a phase-space route to chaos. In fact, more than multistability in the 4D model, we should better speak of the existence of a non-denumerable set of attractors.

For instance, in Figure 8, using the initial conditions in each invariant set $S_{0.9}$, S_0 and Proposition 3, we show in the discontinuous system (8), two symmetric stable periodic orbits that coexist with two symmetric strange attractors.

5 Proofs of the main results

5.1 Proof of Theorems 1 and 2

We start by giving the proof of Theorem 1.

Proof (Proof of Theorem 1) Using remark 1, we can assume the existence of solutions $(x(\tau), y(\tau), z(\tau), w(\tau))$ for which the evaluation of

$$h(\tau) := H(x(\tau), y(\tau), z(\tau), w(\tau))$$

is feasible. Excepting the finite number of points where solutions are not differentiable, after a direct computation, we get that $h'(\tau) = 0$, so that h is at least piecewise constant along the solutions of (2). Since $h(\tau)$ is a continuous function, we obtain that the function is indeed constant everywhere.

Next, we give the proof of Theorem 2

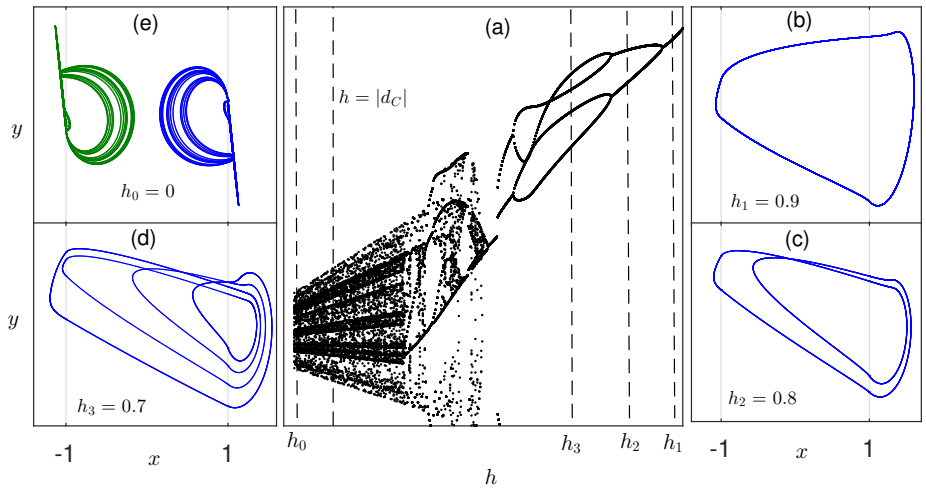

Fig. 7 Simulation results for system (15)-(16) with parameter values as in (25). (a) Plot of the y-coordinate intersection for long term orbits on the Poincaré section $x = 1$ with respect to the parameter h. (b) For $h_1 = 0.9$ we show a stable periodic orbit of three zones. (c) For $h_2 = 0.8$ we have a stable 2-periodic orbit of three zones. (d) For $h_3 = 0.7$ we have a stable 4-periodic orbit of three zones. (e) When $h_0 = 0$ the system has two symmetric strange attractors of two zones.

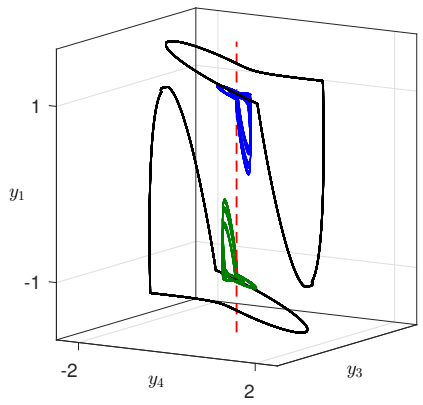

Fig. 8 Simulation results for the discontinuous system (8) obtained by an adequate application of Proposition 3, with parameters values as in (25). The coexistence of two strange attractors along with two stable periodic orbits is shown. The dashed red line represents the unstable equilibrium points.

Proof (Proof of Theorem 2) Solving for y_4 in the equation $H(y_1, y_2, y_3, y_4) = h$ given in (9), we obtain

$$y_4 = \frac{\gamma}{\beta}(y_1 + y_2) - q(y_1) - \frac{1}{\beta}y_3 + \frac{h}{\beta},$$

and substituting this expression in the first three equations of (8), we get

$$\begin{aligned}
\dot{y}_1 &= \frac{\gamma}{\beta}(y_1 + y_2) - q(y_1) - \frac{1}{\beta}y_3 + \frac{h}{\beta},\\
\dot{y}_2 &= y_3 - \frac{\gamma}{\beta}(y_1 + y_2) + q(y_1) + \frac{1}{\beta}y_3 - \frac{h}{\beta},\\
\dot{y}_3 &= -\beta y_2 + \gamma y_3.
\end{aligned} \tag{26}$$

Finally, making the notational change $(x_1, x_2, x_3) = (y_1, y_2, y_3)$, system (26) goes into the form (11).

Remark 3 We note that following a similar procedure to the one done in section 3.1 of [25], it is easy to show how it is possible to get a system equivalent to the continuous reduced system (11), by working from the beginning in the flux-charge setting instead of starting from the discontinuous 4D system (1). This approach is known as Flux-Charge Analysis Method (FCAM, for short) and was proposed in [15].

5.2 Proof of Proposition 2

Remark 4 Note that as a first consequence of theorem 2, when $\beta \neq 0$, $a \neq b$ and the function q is defined as in (13), the dynamics of system (8) on S_h defined in (10) is ruled by a continuous piecewise system of the form

$$\dot{\mathbf{x}} = \begin{cases} A_E\mathbf{x} + \mathbf{b}_C + \mathbf{b}, & \text{if} \quad \mathbf{e}_1^T\mathbf{x} > 1,\\ A_C\mathbf{x} + \mathbf{b}_C, & \text{if} \quad |\mathbf{e_1^T}\mathbf{x}| \leq 1,\\ A_E\mathbf{x} + \mathbf{b}_C - \mathbf{b}, & \text{if} \quad \mathbf{e}_1^T\mathbf{x} < -1, \end{cases} \tag{27}$$

where

$$A_C = \frac{1}{\beta}\begin{pmatrix} \gamma - a\beta & \gamma & -1 \\ a\beta - \gamma & -\gamma & 1+\beta \\ 0 & -\beta^2 & \gamma\beta \end{pmatrix},$$
$$A_E = \frac{1}{\beta}\begin{pmatrix} \gamma - b\beta & \gamma & -1 \\ b\beta - \gamma & -\gamma & 1+\beta \\ 0 & -\beta^2 & \gamma\beta \end{pmatrix}, \quad (28)$$
$$\mathbf{b} = \begin{pmatrix} b-a \\ a-b \\ 0 \end{pmatrix}, \quad \mathbf{b}_C = \frac{h}{\beta}\begin{pmatrix} 1 \\ -1 \\ 0 \end{pmatrix}.$$

Note that in the external zones we have equal matrices representing the linear part. Therefore, system (27)-(28) belongs to the family of quasi-symmetric piecewise linear differential systems, and can be written as (for more details see [9])

$$\dot{\mathbf{x}} = A_E\mathbf{x} + (A_C - A_E)\,\mathbf{e}_1 \mathrm{sat}\left(\mathbf{e}_1^T\mathbf{x}\right) + \mathbf{b}_C, \quad (29)$$

where $\mathrm{sat}\,(x)$ is the normalized saturation function given by

$$\mathrm{sat}\,(x) = \begin{cases} x & \text{if } |x| \le 1, \\ \mathrm{sgn}(x) & \text{if } |x| > 1. \end{cases}$$

The quasi-symmetric piecewise linear system given in (29) can be written in the generalized Liénard's form as we will show in the next theorem. First, we give an auxiliary result.

Proposition 5 *Given any matrix of order* 3 *defined by blocks*

$$A = \begin{pmatrix} a_{11} & \mathbf{r}^T \\ \mathbf{w} & B \end{pmatrix},$$

where

$$\mathbf{r} = \begin{pmatrix} a_{12} \\ a_{13} \end{pmatrix}, \quad \mathbf{w} = \begin{pmatrix} a_{21} \\ a_{31} \end{pmatrix}, \quad B = \begin{pmatrix} a_{22} & a_{23} \\ a_{32} & a_{33} \end{pmatrix},$$

the following statements hold.

(a) The linear invariants of the matrix A can be written as

$$t = a_{11} + \mathrm{tr}\,(B),$$
$$m = \det(B) + a_{11}\mathrm{tr}\,(B) - \mathbf{r}^T\mathbf{w},$$
$$d = a_{11}\det(B) + \mathbf{r}^T B\mathbf{w} - \mathrm{tr}\,(B)\,\mathbf{r}^T\mathbf{w},$$

where t, m and d are the trace, the sum of principal minors and the determinant respectively.

(b) If we consider the matrix

$$G = \begin{pmatrix} 1 & \mathbf{0} \\ \mathbf{s} & Q \end{pmatrix},$$

where $\mathbf{0}$ is a null row vector and

$$\mathbf{s} = \begin{pmatrix} \mathrm{tr}\,(B) \\ \det(B) \end{pmatrix}, \quad Q = \begin{pmatrix} -\mathbf{r}^T \\ \mathbf{r}^T B - \mathrm{tr}\,(B)\,\mathbf{r}^T \end{pmatrix},$$

we have

$$\begin{pmatrix} t & -1 & 0 \\ m & 0 & -1 \\ d & 0 & 0 \end{pmatrix} G = GA$$

Proof Statement (a) can be checked by direct computation. After a direct multiplication we obtain

$$\begin{pmatrix} t & -1 & 0 \\ m & 0 & -1 \\ d & 0 & 0 \end{pmatrix} G = \begin{pmatrix} t - \mathrm{tr}\,(B) & \mathbf{r}^T \\ m - \det(B) & \mathrm{tr}\,(B)\,\mathbf{r}^T - \mathbf{r}^T B \\ d & \mathbf{0} \end{pmatrix},$$

and $GA = (\mathbf{z}, D)$ where the vector $\mathbf{z}$ and the matrix D are given by

$$\mathbf{z} = \begin{pmatrix} a_{11} \\ a_{11}\mathrm{tr}\,(B) - \mathbf{r}^T\mathbf{w} \\ a_{11}\det(B) + \mathbf{r}^T B\mathbf{w} - \mathrm{tr}\,(B)\,\mathbf{r}^T\mathbf{w} \end{pmatrix},$$
$$D = \begin{pmatrix} \mathbf{r}^T \\ \mathrm{tr}\,(B)\,\mathbf{r}^T - \mathbf{r}^T B \\ \mathbf{r}^T\left[B^2 - \mathrm{tr}\,(B)\,B + \det(B)\,I\right] \end{pmatrix}.$$

By Cayley-Hamilton's Theorem, we get $B^2 - \mathrm{tr}\,(B)\,B + \det(B)\,I = \mathbf{0}$, and then statement (b) follows from statement (a).

Theorem 7 *Consider a three-dimensional quasi- symmetric continuous piecewise linear system given by*

$$\dot{\mathbf{x}} = A_E\mathbf{x} + (A_C - A_E)\,\mathbf{e}_1 \mathrm{sat}\left(\mathbf{e}_1^T\mathbf{x}\right) + \mathbf{b}_C, \quad (30)$$

where the column vectors $\mathbf{w}, \mathbf{r} \in \mathbb{R}^2$ and the matrix B are such that

$$A_E = \begin{pmatrix} a_{11} & \mathbf{r}^T \\ \mathbf{w} & B \end{pmatrix}.$$

Assume that the matrix

$$C = \begin{pmatrix} \mathbf{r}^T \\ \mathbf{r}^T B \end{pmatrix} \quad (31)$$

has rank 2, *that is, it is nonsingular. Then, the homeomorphism $\tilde{\mathbf{x}} = G\mathbf{x}$ where*

$$G = \begin{pmatrix} 1 & \mathbf{0} \\ \mathbf{s} & Q \end{pmatrix}, \ \mathbf{s} = \begin{pmatrix} \mathrm{tr}\,(B) \\ \det(B) \end{pmatrix}, \ Q = \begin{pmatrix} -\mathbf{r}^T \\ \mathbf{r}^T B - \mathrm{tr}\,(B)\,\mathbf{r}^T \end{pmatrix} \quad (32)$$

transforms system (30) *into the generalized Liénard's form*

$$\dot{\mathbf{x}} = \begin{pmatrix} t_E & -1 & 0 \\ m_E & 0 & -1 \\ d_E & 0 & 0 \end{pmatrix} \mathbf{x} + \begin{pmatrix} t_C - t_E \\ m_C - m_E \\ d_C - d_E \end{pmatrix} \text{sat}\left(\mathbf{e}_1^T \mathbf{x}\right) + G\mathbf{b}_C, \tag{33}$$

where the tildes for the new variables have been removed, and the parameters t_E, m_E, d_E *and* t_C, m_C, d_C *are the linear invariants (trace, sum of principal minors and determinant) of the matrices* A_E *and* A_C*, respectively.*

Proof From hypothesis, the matrix C has rank 2, so that the matrices Q and then G are nonsingular and the change of variables is well defined. Now, we consider the matrices

$$L_j = \begin{pmatrix} t_j & -1 & 0 \\ m_j & 0 & -1 \\ d_j & 0 & 0 \end{pmatrix} \text{ with } \quad j \in \{E, C\},$$

where t_j, m_j, d_j are the linear invariants (trace, sum of principal minors and determinant) of the matrices A_j with $j \in \{E, C\}$. Since system (30) is continuous, the matrices A_E and A_C satisfy $A_E - A_C = (A_E - A_C)\,\mathbf{e}_1\mathbf{e}_1^T$, where $\mathbf{e}_1$ is the first canonical vector, so that the matrices share the last two columns. From Proposition (5) we have $L_E G = G A_E$ and $L_C G = G A_C$. Thus, we obtain

$$\frac{d\tilde{\mathbf{x}}}{d\tau} = G A_E G^{-1}\tilde{\mathbf{x}} + (L_C - L_E)\, G\mathbf{e}_1 \text{sat}\left(\mathbf{e}_1^T G^{-1}\tilde{\mathbf{x}}\right) + G\mathbf{b}_C.$$

Taking into account that $(L_C - L_E)\, G\mathbf{e}_1 = (L_C - L_E)\,\mathbf{e}_1$ and $\mathbf{e}_1^T G^{-1} = \mathbf{e}_1^T$ we obtain the generalized Liénard's form given in (33) and the theorem follows.

Remark 5 Note that the observability matrix of the system (30) is given by

$$O = \begin{pmatrix} \mathbf{e}_1^T \\ \mathbf{e}_1^T A_E \\ \mathbf{e}_1^T A_E^2 \end{pmatrix} = \begin{pmatrix} 1 & \mathbf{0} \\ a_{11} & \mathbf{r}^T \\ a_{11} + \mathbf{r}^T\mathbf{w} & a_{11}\mathbf{r}^T + \mathbf{r}^T B \end{pmatrix},$$

which has rank 3 if and only if the matrix C has rank 2, so that the assumption made on the matrix C is by no means different from the classical observability condition (see [1]).

Combining Remark 4 and Theorem 7, we obtain the proof of Proposition 2.

Proof (Proof of Proposition 2) From Remark 4, on any invariant manifold S_h the dynamics of system (8) is ruled by a continuous piecewise linear system (27)-(28). Computing the matrix C given in (31) we obtain

$$C = \frac{1}{\beta^2}\begin{pmatrix} \gamma\beta & -\beta \\ \beta^2 - \gamma^2 & \gamma \end{pmatrix},$$

so that $\det(C) = 1/\beta$ and C is nonsingular. From Theorem 7, there exists a matrix G given by

$$G = \frac{1}{\beta}\begin{pmatrix} \beta & 0 & 0 \\ \gamma\beta - \gamma & -\gamma & 1 \\ \beta^2 + \beta - \gamma^2 & \beta - \gamma^2 & \gamma \end{pmatrix}, \tag{34}$$

such that the change of variables $\tilde{\mathbf{x}} = G\mathbf{x}$ transforms system (27)-(28) into the Generalized Liénard's form (15) and the conclusion follows.

Remark 6 If $\mathbf{y}(\tau) = (y_1(\tau), y_2(\tau), y_3(\tau), y_4(\tau))$, is a solution of system (8), from Theorem 1 we obtain the constant value

$$h = H(y_1(\tau), y_2(\tau), y_3(\tau), y_4(\tau)), \tag{35}$$

where H is given in (9), so that $\mathbf{y}(\tau) \in S_h$. From Theorem 2, for h given in (35) we get that $\mathbf{x}(\tau) = G(y_1(\tau), y_2(\tau), y_3(\tau))^T$ is a solution of the canonical system (15)-(16) where the matrix G is given in (34). The eigenvalues of the matrices A_E and A_C are the roots of the polynomials $p_j(\lambda) = \lambda^3 - t_j\lambda^2 + m_j\lambda - d_j$ with $j \in \{E, C\}$.

Proof (Proof of Proposition 3) Assume that $\mathbf{x}(\tau) = (x_1(\tau), x_2(\tau), x_3(\tau)) \in \mathbb{R}^3$ is a solution of the canonical system (15)-(16) for some $h \in \mathbb{R}$. From Theorem 2 there exists a nonsingular matrix G such that $G^{-1}\mathbf{x}(\tau)$ is a solution of the non-canonical system (11). Taking into account that

$$\begin{pmatrix} y_1(\tau) \\ y_2(\tau) \\ y_3(\tau) \end{pmatrix} = G^{-1}\mathbf{x}(\tau),$$

we obtain the three first components given in (17), and defining

$$y_4(\tau) = \frac{\gamma}{\beta}(y_1(\tau) + y_2(\tau)) - q(y_1(\tau)) - \frac{1}{\beta}y_3(\tau) + \frac{h}{\beta} = \\ = \gamma x_1(\tau) - x_2(\tau) - q(x_1(\tau)) + \frac{h}{\beta},$$

we obtain trivially $H(y_1(\tau), y_2(\tau), y_3(\tau), y_4(\tau)) = h$, where H is given in (9), that is $\left(G^{-1}\mathbf{x}(\tau), y_4(\tau)\right) \in S_h$. Now, after to direct computation we get $\dot{y}_1 = y_4, \quad \dot{y}_2 = y_3 - y_4, \quad \dot{y}_3 = -\beta y_2 + \gamma y_3$ and taking into account that $\dot{y}_1 + \dot{y}_2 = y_3$ we obtain

$$\dot{y}_4 = \frac{\gamma}{\beta}(\dot{y}_1 + \dot{y}_2) - W(y_1(\tau))\dot{y}_1 - \frac{1}{\beta}\dot{y}_3 = \\ = y_2(\tau) - W(y_1(\tau))y_4(\tau).$$

Thus $\mathbf{y}(\tau)$ defined as in (17) is a solution of discontinuous system (8) and the conclusion follows.

5.3 Proof of Proposition 4

In the following result we study the existence of real equilibrium points and their transitions between the central zone and the externals zones. The proof is a direct computation and is omitted.

Proposition 6 *Consider canonical system* (15)-(16) *with* $a \neq b$. *The following statements hold.*

(a) The system has for $|h| \leq |d_C|$ *one real equilibrium point in the central zone* $\left|\mathbf{e}_1^T\mathbf{x}\right| \leq 1$, *with coordinates*

$$\mathbf{x}_C^* = h\begin{pmatrix} -\frac{1}{d_C} \\ \frac{1}{\beta} - \frac{t_C}{d_C} \\ \frac{\gamma}{\beta} - \frac{m_C}{d_C} \end{pmatrix}. \tag{36}$$

(b) For $\frac{h+d_C}{d_E} < 0$ *the system has one real equilibrium point in the right external zone* $\mathbf{e}_1^T\mathbf{x} > 1$, *with coordinates*

$$\mathbf{x}_R^* = \begin{pmatrix} 1 - \frac{h+d_C}{d_E} \\ t_C - \frac{t_E}{d_E}d_C + \left(\frac{1}{\beta} - \frac{t_E}{d_E}\right)h \\ m_C - \frac{m_E}{d_E}d_C + \left(\frac{\gamma}{\beta} - \frac{m_E}{d_E}\right)h \end{pmatrix}. \tag{37}$$

(c) For $\frac{h-d_C}{d_E} > 0$ *the system has one real equilibrium point in the left external zone* $\mathbf{e}_1^T\mathbf{x} < -1$, *with coordinates*

$$\mathbf{x}_L^* = \begin{pmatrix} -1 - \frac{h-d_C}{d_E} \\ -t_C + \frac{t_E}{d_E}d_C + \left(\frac{1}{\beta} - \frac{t_E}{d_E}\right)h \\ -m_C + \frac{m_E}{d_E}d_C + \left(\frac{\gamma}{\beta} - \frac{m_E}{d_E}\right)h \end{pmatrix}. \tag{38}$$

Proof (Proof of Proposition 4) From Proposition 6 we have

$$\mathbf{e}_1^T\mathbf{x}_C^* = -\frac{h}{d_C}, \quad \mathbf{e}_1^T\mathbf{x}_L^* = -1 + \frac{d_C}{d_E} - \frac{h}{d_E},$$
$$\mathbf{e}_1^T\mathbf{x}_R^* = 1 - \frac{d_C}{d_E} - \frac{h}{d_E},$$

where $\mathbf{e}_1$ is the canonical vector. Assuming that $d_C > 0$ and $d_E < 0$ we obtain

$$\begin{aligned} &|\mathbf{e}_1^T\mathbf{x}_C^*| \leq 1, \quad \text{for } -d_C \leq h \leq d_C, \\ &\mathbf{e}_1^T\mathbf{x}_R^* > 1, \quad \text{for } -d_C < h, \\ &\mathbf{e}_1^T\mathbf{x}_L^* < -1, \quad \text{for } h < d_C. \end{aligned}$$

Thus, for $|h| < d_C$ the system has three real equilibrium points while for $h = d_C$ we get $\mathbf{e}_1^T\mathbf{x}_C^* = \mathbf{e}_1^T\mathbf{x}_L^*$, so that the system has two equilibrium points and passing through at $h = d_C$ we have a non-smooth fold boundary equilibrium bifurcation. Analogously, for $h = -d_C$ we have $\mathbf{e}_1^T\mathbf{x}_C^* = \mathbf{e}_1^T\mathbf{x}_R^*$. The case $d_C < 0$ and $d_E > 0$ is analogous and statement (a) follows.

If $d_C > 0$ and $d_E > 0$ the system has only one real equilibrium point for any $h \in R$ so that there exists a persistence of the equilibrium point at $h = d_C$ and $h = -d_C$. The case $d_C < 0$ and $d_E < 0$ is analogous and the proof is completed.

Note that, the above BEB's could be detected by applying Theorem 5.1 of [6] or [17], but here is not necessary thanks to the canonical form (15)-(16) which facilitates the required computations.

When the equilibria are not at the boundaries $|\mathbf{e}_1^T\mathbf{x}| = 1$, their stability can be obtained by standard criteria, as follows.

Proposition 7 *Consider system* (15)-(16) *with* $a \neq b$, $|h| \neq |d_C|$ *and the equilibrium points given in* (36)-(37)-(38). *The following statements hold.*

(a) When equilibrium point $\mathbf{x}_C^*$ *is real, it will be asymptotically stable if* $t_C < 0$, $d_C < 0$ *and* $m_C t_C - d_C < 0$, *that is*

$$\gamma - a < 0, \quad \gamma - a\beta < 0, \quad a^2\gamma - a\gamma^2 + \beta\gamma - a < 0.$$

(b) When a external equilibrium point ($\mathbf{x}_R^*$ *or* $\mathbf{x}_L^*$*) is real, it will be asymptotically stable if* $t_E < 0$, $d_E < 0$ *and* $m_E t_E - d_E < 0$, *that is*

$$\gamma - b < 0, \quad \gamma - b\beta < 0, \quad b^2\gamma - b\gamma^2 + \beta\gamma - b < 0.$$

Proof The matrices $A_{C,E}$ have the characteristic polynomial

$$p_j(\lambda) = \lambda^3 - t_j\lambda^2 + m_j\lambda - d_j, \quad \text{with} \quad j \in \{E, C\}.$$

Thus, by a direct application of the Routh-Hurwitz Theorem we obtain $t_j < 0$, $d_j < 0$, $m_j t_j < d_j$ and both statements follows.

However, when the equilibria are at the boundaries $|\mathbf{e}_1^T\mathbf{x}| = 1$, their stability is a problem much more involved. In particular, as shown in [11], it is possible to have an unstable equilibrium point even when the two matrices A_C and A_E are Hurwitzian. The difficulties arise from the possible existence of invariant cones where the dynamics is not easy to control, see for more details [10].

5.4 Proof of Theorems 4 and 5

In order to show Theorems 4 and 5, we show first some auxiliary results. Assuming β fixed, we start by analyzing the auxiliary expression $\varepsilon(a, \gamma) = m_C t_C - d_C$ that leads to the bifurcation when it vanishes, where m_C, t_C and d_C are given in (16).

For $\beta \neq 1$, the condition $\varepsilon(a,\gamma)=0$ is equivalent to $a\gamma\,(a-\gamma)=a-\beta\gamma$, which is only possible for $a\gamma>0$, so that the points where (19) vanishes are in the first or third quadrant of the parameter plane (a,γ). The following Lemma is direct and so we omit its proof.

Lemma 1 *Consider for the reduced system* (15)-(16) *the auxiliary expression* (19)*, where t_C, m_C and d_C are given in* (16) *and $a>0$, $\beta\neq 1$. The following statements hold.*

(a) The points of the parameter plane (a,γ) where ε vanishes satisfy $\gamma\neq a$.

(b) If $0<\beta<1$ then $\left(\gamma^2+1\right)^2>4\beta\gamma^2$ and we have the factorization

$$\varepsilon(a,\gamma)=\gamma\,(a-a_+(\gamma))\,(a-a_-(\gamma))\,, \tag{39}$$

where

$$a_\pm(\gamma)=\frac{\gamma^2+1}{2\gamma}\pm\sqrt{\left(\frac{\gamma^2+1}{2\gamma}\right)^2-\beta}, \tag{40}$$

so that $a_-(\gamma)<\gamma<a_+(\gamma)$. Thus at the points $(a_-(\gamma),\gamma)$ we have $t_C>0$ and $d_C>0$, while for $(a_+(\gamma),\gamma)$ we have $t_C<0$. Furthermore, for $\gamma<\sqrt{\beta(1+\beta)}$ we also have $\gamma<a_+(\gamma)\beta$, that is, $d_C<0$ at such points $(a_+(\gamma),\gamma)$, see Figure 3 (a).

(c) If $\beta>1$ then $\beta+a^2>2a$ and we have the factorization

$$\varepsilon(a,\gamma)=-a\,(\gamma-\gamma_+(a))\,(\gamma-\gamma_-(a))\,, \tag{41}$$

where

$$\gamma_\pm(a)=\frac{a^2+\beta}{2a}\pm\sqrt{\left(\frac{a^2+\beta}{2a}\right)^2-1}, \tag{42}$$

so that $\gamma_-(a)<a<\gamma_+(a)$. Thus at the points $(a,\gamma_-(a))$ we have $t_C<0$ and $d_C<0$, while for $(a,\gamma_+(a))$ we have $t_C>0$. Furthermore, for $a<\sqrt{(1+\beta)/\beta}$ we also have $a\beta<\gamma_+(a)$, that is $d_C>0$ at such points $(a,\gamma_+(a))$, see Figure 3 (b).

Remark 7 Regarding conditions (18), we need in the bifurcation that $\mathrm{sgn}(t_C)=\mathrm{sgn}(d_C)$. Therefore, we note that for $\beta>1$ the points on the curve $\varepsilon(a,\gamma)=0$ with $a<\gamma<a\beta$ do not represent FCLC bifurcation points. Analogously, for $\beta<1$ we must neglect the points with $a\beta<\gamma<a$.
The point (a,γ) at the curve $\varepsilon(a,\gamma)=0$ with $\gamma=a\beta$ namely

$$DZ=\left(\sqrt{\frac{1+\beta}{\beta}},\sqrt{\beta\,(1+\beta)}\right), \tag{43}$$

represents a higher codimension bifurcation point (a double zero, since $d_C=m_C=0$) from which the curve of FCLC bifurcation emanates (see Figure 3).

In the next Lemma we study the sign of parameters m_C and ρ on the bifurcation curve $\varepsilon(a,\gamma)=0$, in order to apply Theorem 3.

Lemma 2 *Consider the canonical system* (15)-(16) *with $|h|<|d_C|\neq 0$ and $a\neq b$, where we also assume $a,\gamma>0$, $0<\beta\neq 1$ and ε given in* (19)*. The following statements hold.*

(a) For m_C and ρ defined in (16) *and* (21) *respectively, we have*

$$\begin{aligned} m_0 &:= m_C|_{f=0}=\frac{\gamma-\beta a}{\gamma-a},\\ \rho_0 &:= \rho|_{f=0}=m_0\frac{\gamma\,(b-a)}{a}\left(\beta-a^2\right). \end{aligned} \tag{44}$$

(b) When $m_0\neq 0$ and $\beta<1$, we have $\rho_0\neq 0$.

(c) When $m_0\neq 0$ and $\beta>1$ there exist two points at the bifurcation curve given by

$$p_\pm=\left(\sqrt{\beta},\sqrt{\beta}\pm\sqrt{\beta-1}\right), \tag{45}$$

such that $\rho_0(p_\pm)=0$.

Proof To show statement (a), we note that $\varepsilon(a,\gamma)=0$ is equivalent to $d_C=m_Ct_C$, so that the expression for m_0 is direct. Also, on the curve $\varepsilon(a,\gamma)=0$, we have

$$\gamma^2+1=\frac{\gamma}{a}\left(a^2+\beta\right). \tag{46}$$

Now, we obtain from (21)

$$\rho|_{f=0}=m_0\left(d_C-m_Et_C+d_E-m_0t_E\right).$$

Using (46) and after some algebra we obtain

$$\begin{aligned} d_C-m_Et_C+d_E-m_Ct_E &= \frac{\gamma\,(a^2+\beta)}{a}\,(a+b)-2\gamma\,(ab+\beta)=\\ &=\frac{\gamma}{a}\,(b-a)\left(\beta-a^2\right), \end{aligned}$$

and the statement (a) follows.
If $m_0\neq 0$ and in (44) we assume $a^2=\beta$, from (19) we get that $\varepsilon(a,\gamma)=0$ is equivalent to the condition $\gamma^2+1=2a\gamma$, so that for all $\gamma>0$ we have

$$a=\frac{\gamma^2+1}{2\gamma}=\frac{1}{2}\left(\gamma+\frac{1}{\gamma}\right)>1, \tag{47}$$

which implies $\beta>1$, getting a contradiction. Statement (b) follows.
Finally, if $m_0\neq 0$ the only posibility for $\rho_0=0$ is $a^2=\beta>1$. From (42) we obtain $\gamma_\pm(\sqrt{\beta})=\sqrt{\beta}\pm\sqrt{\beta-1}$ and the lemma follows.

Remark 8 According to Remark 7 the point p_+ given in (45) must be neglected when at such point $a < \gamma < a\beta$

$$\sqrt{\beta} < \sqrt{\beta} + \sqrt{\beta - 1} < \beta\sqrt{\beta},$$

and this fails when $\sqrt{\beta} + \sqrt{\beta - 1} > \beta\sqrt{\beta}$. Multiplying by $\sqrt{\beta} - \sqrt{\beta - 1} > 0$ and after some algebra, we obtain the equivalent inequality

$$0 > \beta^3 - 2\beta^2 + 1 = (\beta - 1)(\beta - \phi)\left(\beta + \frac{1}{\phi}\right),$$

where $\phi = \frac{1+\sqrt{5}}{2}$ is the golden ratio. Thus, for $\beta > \phi$, the point p_+ lies on the portion of the curve $\gamma = \gamma_+(a)$ that does not represents FCLC bifurcation points.

Proof (Proof of Theorem 4) Under the hypothesis $\beta < 1$, the points in the branch $(a, \gamma) = (a_-(\gamma), \gamma)$ satisfy $a_-(\gamma)\beta < a_-(\gamma) < \gamma$ and $m_0 > 0$ from (44). Furthermore, we know from statement (b) of Lemma 2 that the sign of ρ_0 does not change for all the points of the branch. To discriminate this sign, from (44) we only need to check the sign of $\beta - a^2$. Taking $\gamma = 1$, we see after some algebra that $\beta > a_-(1)^2 = \left(1 - \sqrt{1-\beta}\right)^2$ and so $\rho_0 > 0$. The conclusion follows from Theorem 3, since $a < a_+(\gamma)$ and

$$\varepsilon(a, \gamma) = \gamma\,(a - a_+(\gamma))\,(a - a_-(\gamma)) > 0$$

for $a - a_-(\gamma) < 0$ indicating that the limit cycle appears for $a < a_-(\gamma)$ and is unstable since $a_-(\gamma)\beta < \gamma$ and so $d_C > 0$. Statement (a) follows.
Analogously, we know that only for $\gamma < \sqrt{\beta(1+\beta)}$ the points in the branch $(a, \gamma) = (a_+(\gamma), \gamma)$ satisfy $\gamma < a_+(\gamma)\beta < a_+(\gamma)$ and so $m_0 > 0$ from (44). The sign of the ρ_0 will also be determined by the sign of $\beta - a^2$. Taking $\gamma = 1$, we see that $\beta - (1 + \sqrt{1-\beta})^2 < 0$ and so $\rho_0 < 0$. So that the bifurcation does not involve stable limit cycles. In this branch we have $a - a_-(\gamma) > 0$, then the limit cycle bifurcates for $a < a_+(\gamma)$ and it is unstable although $d_C = \gamma - a_+(\gamma)\beta < 0$, according to Theorem 3.
To show statement (c) we start with the case $a < \sqrt{\beta}$, that is, on the left of point p_-, see Figure 3(b). Then, we have that $\gamma_-(a) < a < a\beta$, so that from (44) we get that $m_0 > 0$. Then, under our hypothesis $a < \sqrt{\beta}$ we deduce that $\rho_0 > 0$ and then the bifurcating limit cycle predicted by Theorem 3 will appear for $\gamma > \gamma_-(a)$, since $\varepsilon(a, \gamma) = -a\,(\gamma - \gamma_+(a))\,(\gamma - \gamma_-(a))$ and $\gamma - \gamma_+(a) < 0$. The stability comes from the inequalities $\rho_0 > 0$ and $d_C < 0$. The case $a > \sqrt{\beta}$ is the dual case where $\rho_0 < 0$ and the bifurcation appears for $\gamma < \gamma_-(a)$ leading to an unstable limit cycle.
To show statement (d) we consider first the case $a < \sqrt{\beta}$. Now, from statement (c) of Lemma 1, we have $a < a\beta < \gamma_+(a)$ and so $m_0 > 0$. Here $\rho_0 > 0$, and as $\gamma - \gamma_-(a) < 0$, the limit cycle bifurcates for $\gamma > \gamma_+(a)$ but it is unstable because $d_C = \gamma - a\beta > 0$. The case $\sqrt{\beta} < a < \sqrt{(1+\beta)/\beta}$, which is only possible when $\beta < \phi$, is the dual case with $\rho_0 < 0$, also leading to an completely unstable limit cycle.
Regarding statement (e), we see that

$$a^2 < \frac{1+\beta}{\beta} = 1 + \frac{1}{\beta} \leq 1 + \frac{1}{\phi} = \phi \leq \beta,$$

so that $\rho_0 < 0$ as before, along with $d_C > 0$, and the Theorem follows.

The proof of the Theorem 5 is analogous and so it is omitted.

6 Conclusions

Taking advantage of the discovered conserved quantity in the 4D canonical memristor oscillators proposed by M. Itoh & L. Chua, we have been able to formulate reduced 3D models that allow to reproduce the complex dynamics of such devices. Furthermore, the sudden generation of a hypersurface foliated by stable periodic orbits has been completely characterized for the four-parameter set of the system. This gives a remarkable first occurrence of what can be called multiple center-cycle bifurcation, a rich phenomenon non reported in the literature. Several numerical simulations, also included in the paper, not only confirm the theoretical results achieved but also stimulate future research by showing similar and even more complicated dynamics in the studied 4D memristor oscillators.

7 Acknowledgments

Andrés Amador is supported by *Pontificia Universidad Javeriana Cali-Colombia*. Enrique Ponce and Javier Ros are partially supported by the Spanish *Ministerio de Economía y Competitividad*, in the frame of project MTM2015-65608-P, and by the *Consejería de Economía y Conocimiento de la Junta de Andalucía* under grant P12-FQM-1658.

Compliance with ethical standards: Conflict of Interest

The authors declare that they have no conflict of interest.

References

1. Afanasiev, V., Kolmanovskii, V., Nosov, V.: Mathematical Theory of Control Systems Design, 1 edn. Springer Netherlands (1996)
2. Amador, A., Freire, E., Ponce, E., Ros, J.: On discontinuous piecewise linear models for memristor oscillators. International Journal of Bifurcation and Chaos **27**(06), 1730,022–1730,040 (2017)
3. Bao, B., Bao, H., Wang, N., Chen, M., Xu, Q.: Hidden extreme multistability in memristive hyperchaotic system. Chaos, Solitons & Fractals **94**(Supplement C), 102–111 (2017)
4. Bao, B., Tao, J., Xu, Q., Chen, M., Wu, H., Hu, Y.: Coexisting infinitely many attractors in active band-pass filter-based memristive circuit. Nonlinear Dyn **86**, 1711–1723 (2016)
5. Bao, H., Jiang, T., Chu, K., Chen, M., Xu, Q., Bao, B.: Memristor-based canonical chua's circuit: Extreme multistability in voltage-current domain and its controllability in flux-charge domain. Complexity **2018**, 1–13 (2018)
6. Bernardo, M., Budd, C., Champneys, A.R., Kowalczyk, P.: Piecewise-smooth Dynamical Systems, 1 edn. Springer-Verlag London (2008)
7. di Bernardo, M., Nordmark, A., Olivar, G.: Discontinuity-induced bifurcations of equilibria in piecewise-smooth and impacting dynamical systems. Physica D: Nonlinear Phenomena **237**(1), 119 – 136 (2008)
8. Carmona, V., Freire, E., Ponce, E., Ros, J., Torres, F.: Limit cycle bifurcation in 3D continuous piecewise linear systems with two zones: Application to Chua's circuit. International Journal of Bifurcation and Chaos **15**(10), 3153–3164 (2005)
9. Carmona, V., Freire, E., Ponce, E., Torres, F.: On simplifying and classifying piecewise-linear systems. IEEE Trans. Circuits and Systems. I **49**(5), 609–620 (2002)
10. Carmona, V., Freire, E., Ponce, E., Torres, F.: Bifurcation of invariant cones in piecewise linear homogeneous systems. International Journal of Bifurcation and Chaos **15**(08), 2469–2484 (2005)
11. Carmona, V., Freire, E., Ponce, E., Torres, F.: The continuous matching of two stable linear systems can be unstable. Discrete and Continuous Dynamical Systems **16**(3), 689–703 (2006)
12. Chen, H., Li, X.: Global phase portraits of memristor oscillators. International Journal of Bifurcation and Chaos **24**(12), 1450,152 (2014)
13. Chen, M., Sun, M., Bao, B., Wu, H., Xu, Q., Wang, J.: Controlling extreme multistability of memristor emulator-based dynamical circuit in flux–charge domain. Nonlinear Dynamics **91**(2), 1395–1412 (2017)
14. Chua, L.O.: Memristor: The missing circuit element. IEEE Trans. Circuit Theory **18**, 507–519 (1971)
15. Corinto, F., Forti, M.: Memristor circuits: Flux-charge analysis method. IEEE Transactions on Circuits and Systems I: Regular Papers **63**(11), 1997–2009 (2016)
16. Corinto, F., Forti, M.: Memristor circuits: Bifurcations without parameters. IEEE Transactions on Circuits and Systems I: Regular Papers **64**(6), 1540–1551 (2017)
17. Di Bernardo, M., Pagano, D.J., Ponce, E.: Nonhyperbolic boundary equilibrium bifurcations in planar Filippov systems: A case study approach. International Journal of Bifurcation and Chaos **18**(05), 1377–1392 (2008)
18. Filippov, A.: Differential Equations with Discontinuous Righthand Sides, 1 edn. Springer Netherlands (1988)
19. Freire, E., Ordoñez, M., Ponce, E.: Limit cycle bifurcation from a persistent center at infinity in 3D piecewise linear systems with two zones. In: Colombo A., Jeffrey M., Lázaro J., Olm J. (eds) Extended Abstracts Spring 2016. Trends in Mathematics, vol 8. Birkhäuser, Cham (2017)
20. Freire, E., Ponce, E., Ros, J.: The focus-center-limit cycle bifurcation in symmetric 3D piecewise linear systems. SIAM J. Appl. Math **65**(6), 1933–1951 (2005)
21. Freire, E., Ponce, E., Ros, J.: Bistability and hysteresis in symmetric 3D piecewise linear oscillators with three zones. International Journal of Bifurcation and Chaos **18**(12), 3633–3645 (2008)
22. Freire, E., Ponce, E., Ros, J.: Following a saddle-node of periodic orbits bifurcation curve in Chua's circuit. International Journal of Bifurcation and Chaos **19**(02), 487–495 (2009)
23. Itoh, M., Chua, L.O.: Memristor oscillators. International Journal of Bifurcation and Chaos **18**(11), 3183–3206 (2008)
24. Kengne, J., Negou, A.N., Tchiotsop, D.: Antimonotonicity, chaos and multiple attractors in a novel autonomous memristor-based jerk circuit. Nonlinear Dyn **88**, 2589–2608 (2017)
25. Ponce, E., Ros, J., Freire, E., Amador, A.: Unravelling the dynamical richness of 3D canonical memristor oscillators. Microelectronic Engineering **182**, 15–24 (2017)
26. Ponce, E., Ros, J., Vela, E.: Unfolding the fold-Hopf bifurcation in piecewise linear continuous differential systems with symmetry. Physica D: Nonlinear Phenomena **250**, 34–46 (2013)
27. Simpson, D.: The instantaneous local transition of a stable equilibrium to a chaotic attractor in piecewise-smooth systems of differential equations. Physics Letters A **380**(38), 3067–3072 (2016)
28. Strukov, D.B., Snider, G.S., Stewart, G.R., Williams, R.S.: The missing memristor found. Nature **453**, 80–83 (2008)
29. Tucker, W.: Computing accurate Poincaré maps. Physica D: Nonlinear Phenomena **171**(3), 127–137 (2002)
30. Wang, G., Yuan, F., Chen, G., Zhang, Y.: Coexisting multiple attractors and riddled basins of a memristive system. Chaos: An Interdisciplinary Journal of Nonlinear Science **28**(1), 013,125 (2018)
31. Wang, Z., Akgul, A., Pham, V.T., Jafari, S.: Chaos-based application of a novel no-equilibrium chaotic system with coexisting attractors. Nonlinear Dynamics **89**(3), 1877–1887 (2017)
32. Yuan, F., Wang, G., Wang, X.: Extreme multistability in amemristor-based multi-scroll hyper-chaotic system. Chaos **26**(7), 073,107 (2017)
33. Zhang, S., Zeng, Y., Li, Z., Wang, M., Xiong, L.: Generating one to four-wing hidden attractors in a novel 4d no-equilibrium chaotic system with extreme multistability. Chaos: An Interdisciplinary Journal of Nonlinear Science **28**(1), 013,113 (2018)
34. Zheng, C., Iu, H.H.C., Fernando, T., Yu, D., Guo, H., Eshraghian, J.K.: Analysis and generation of chaos using compositely connected coupled memristors. Chaos: An Interdisciplinary Journal of Nonlinear Science **28**(6), 063,115 (2018)